Eur. Phys. J. C (2023) 83:820
https://doi.org/10.1140/epjc/s10052-023-12012-w

THE EUROPEAN PHYSICAL JOURNAL C

Regular Article - Theoretical Physics

Hidden charmonium decays of $\psi(nS)$ through charmed meson loops

Shidong Liu[1], **Zuxin Cai**[1], **Yuanxin Zheng**[1], **Gang Li**[1,2,a]

[1] College of Physics and Engineering, Qufu Normal University, Qufu 273165, China
[2] CAS Key Laboratory of Theoretical Physics, Institute of Theoretical Physics, Chinese Academy of Sciences, Beijing 100190, China

Received: 17 July 2023 / Accepted: 5 September 2023 / Published online: 13 September 2023

Abstract We calculated transitions of the higher radial excited charmonia $\psi(nS)$ $(n = 3, 4, 5)$ to the orbital excited charmonium $h_c(1P)$ with emission of one pion or eta meson. In calculations, the intermediate S- and P-wave charmed meson loops were considered in terms of the nonrelativistic effective field theory. The results indicate that the transitions of interest are dominated by the loops involving the $s_l^P = (1/2)^+$ charmed mesons, whereas the $s_l^P = (1/2)^-$ charmed meson loops are of minor contributions. The partial decay widths of $\psi(nS) \to h_c\pi^0$ are of the order of 0.01–1 keV. For the case of $\psi(nS) \to h_c\eta$, the partial decay widths are from 0.1 to 100 keV, implying the branching ratios from 10^{-5} to 10^{-3}. Moreover, the partial decay widths for $\psi(nS) \to h_c\eta$ are found to decrease as the η-η' mixing angle increases. It is hoped that the present calculated results would be observed in the future experiments.

1 Introduction

Decays of the heavy quarkonia can give valuable insights into quantum chromodynamics (QCD), the theory of the strong interactions, in both the perturbative and non-perturbative regimes [1–3]. Up to now, it has accumulated huge data samples for the heavy quarkonium decays by various experiments in the world, as summarized in the Review of Particle Data Group [4]. These experimental observations provide us a basic understanding of the quarkonium physics, but there still remain many mysteries in charmonium physics to be settled. Moreover, a number of theoretical tools (e.g., Quark and potential models [5], Effective field theories [6], Lattice gauge theory approaches [7]) have been developed to give further interpretations. In the $c\bar{c}$ sector, apart from the ordinary hadrons in terms of the quark model, many exotic states, usually referred to as XYZ states, with different properties from the quark-model expectations have been observed in numerous experiments. Many theoretical investigations have been carried out in order to understand their nature (see Refs. [8,9] for reviews).

Numerous calculations provide evidence that the intermediate meson loops play an important role in the decays of charmonia [10–33]. It indicates that for the J/ψ decaying into the light pseudoscalar and vector mesons the meson loops have a comparable contribution to that from the single-OZI process [10]. The importance of the meson loops is also revealed in the magnetic dipole transitions of the J/ψ and $\psi(2S)$, namely $J/\psi \to \gamma\eta_c$ and $\psi(2S) \to \gamma\eta_c(\gamma\eta_c')$ [12,23]. To better understand the puzzle charmonium exclusive decays (e.g., the celebrated $\psi(3770)$ non-$D\bar{D}$ decays and $\rho\pi$ puzzle), the effects of the meson loops appear to be one of the possible interpretations [17,34,35]. Furthermore, the properties of some charmoniumlike states, for instance the $Y(4260)$, could be studied using the meson loops [36–38].

The hadronic transitions with one pion or eta meson emission between two charmonia of mass smaller than ~ 4.0 GeV have been systematically investigated by Guo et al. [20,21]. That work was primarily based on a nonrelativistic effective field theory [19]. For the transitions between two S-wave or two P-wave charmonia the intermediate charmed meson loops give dominant contributions compared with the tree-level ones. However, for some transitions between one S-wave and one P-wave charmonia, especially for the transition $\psi(2S) \to h_c\pi^0$, the charmed meson loops are found to be strongly suppressed and the tree-level contributions are of absolute dominance. The suppression is partly due to the rather small phase space [20]. Additionally, only the P-wave couplings of the initial $\psi(2S)$ or the final pion to a pair of charmed mesons with $s_l^P = (1/2)^-$ were considered in the early work [20,21], which would also suppress the loop

[a] e-mail: gli@qfnu.edu.cn (corresponding author)

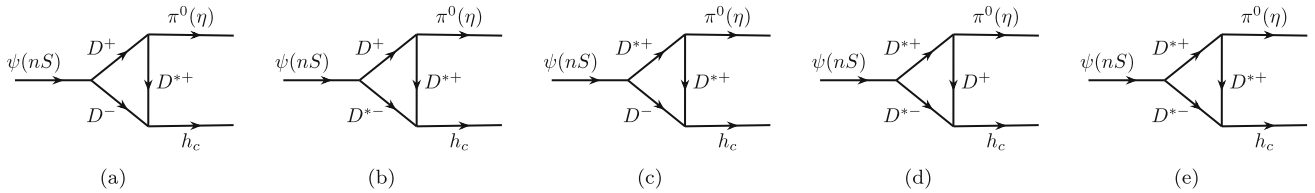

Fig. 1 The hadron-level diagrams for the transitions $\psi(nS) \to h_c\pi^0(\eta)$ through the charged charmed meson loops. The neutral charmed meson loops can be obtained by changing the charged mesons into the corresponding neutral ones. In the same way, we could get the loops composed of the D_s mesons only for the processes $\psi(nS) \to h_c\eta$

contributions. Hence, if we consider the higher radial excited charmonia that lead to relatively large phase spaces and open the $D\bar{D}$ threshold, the suppression would be weakened. Furthermore, when the $(1/2)^-$ charmed meson connecting the initial charmonia and the final light meson (π^0) is replaced by the $(1/2)^+$ charmed meson, the corresponding couplings would occur in a S-wave, thereby enhancing the loop contributions.

In this work, we calculated, using the nonrelativistic effective field theory, the hadronic transitions with one pion or eta meson emission from the higher radial excited charmonia $\psi(nS)$ ($n = 3, 4, 5$) to the P-wave charmonium $h_c(1P)$. In the calculations, we considered both the S- and P-wave charmed meson loop contributions. As mentioned above, compared with the suppressed transitions $\psi(2S) \to h_c\pi^0(\eta)$, the present transitions we consider have relatively large phase spaces, thereby partly weakening the suppression. Moreover, the triangular loops comprised of three S-wave vertices were included in our calculations. As a consequence, the charmed meson loop contributions would become more important again. Our calculations presented in the following bear this out.

The rest of the paper is organized as follows. In Sect. 2, we present the theoretical framework used in this work. Then in Sect. 3 the numerical results are presented, and a brief summary is given in Sect. 4.

2 Theoretical considerations

The numerical calculations in the framework of nonrelativistic effective field theory used here are basically similar to those [19–21] that turn out to be adequate for the heavy quarkonium transitions through the corresponding open quark mesons [8,19–22,39,40]. In the present calculations, we consider the contribution of the S- and P-wave intermediate charmed meson loops. We exhibit in Fig. 1 the Feynman diagrams of the charged charmed meson loops for the transition processes $\psi(nS) \to h_c\pi^0(\eta)$. The loops made of the neutral or strange charmed mesons are not shown here, but included in our calculations.

In the case of transitions between the radial and orbital excited charmonia, we could describe the charmonium fields using the two-component notation. The representation for the S-wave charmonium fields is

$$J = \vec{\psi} \cdot \vec{\sigma} + \eta_c \,, \tag{1}$$

where $\vec{\sigma}$ are Pauli sigma matrices, and $\vec{\psi}$ and η_c indicate the annihilation of the ψ and η_c states, respectively.

The fields for the pseudoscalar (P_a) and vector ($\vec{V}_a$) charmed mesons made of heavy and light quarks of $s_l^P = (1/2)^-$ are written together as

$$H_a = \vec{V}_a \cdot \vec{\sigma} + P_a \,. \tag{2}$$

Here the subscript a indicates the light flavor. In terms of the light quark, $P_a = (D^0, D^+, D_s^+)$ and $\vec{V}_a = (D^{*0}, D^{*+}, D_s^{*+})$. Apart from the $s_l^P = (1/2)^-$ charmed mesons, we also take the $s_l^P = (1/2)^+$ states into account. In an analogous manner, such field is expressed by

$$S_a = \vec{V}_{1a} \cdot \vec{\sigma} + P_{0a}^* \,, \tag{3}$$

with $\vec{V}_{1a} = (D_1^0, D_1^+, D_{s1}^+)$ and $P_{0a}^* = (D_0^*, D_0^{*+}, D_{s0}^{*+})$. As an illustration, three intermediate meson loops involving the D_1^0 and D_0^* are shown in Fig. 2. Since the $D_1^\pm$ and $D_0^{*\pm}$ have not been discovered, we assumed that the mass difference between $D_1^\pm(D_0^{*\pm})$ and $D_1^0(D_0^*)$ follows the relation [4]

$$\begin{aligned} m_{D_1^\pm} - m_{D_1^0} &= m_{D_0^{*\pm}} - m_{D_0^*} \\ &= \frac{1}{2}\left[(m_{D^\pm} - m_{D^0}) + (m_{D^{*\pm}} - m_{D^{*0}})\right] = 4.116\ \text{MeV}. \end{aligned} \tag{4}$$

In view of the parity, charge conjugation, and spin symmetry, the leading order Lagrangian involving an S-wave charmonium and a pair of charmed and anticharmed mesons is given by

$$\mathcal{L}_\psi = \mathrm{i}\frac{g_1}{2}\langle \bar{H}_a^\dagger \vec{\sigma} \cdot \overleftrightarrow{\partial} H_a^\dagger J\rangle + g_1'\langle(\bar{H}_a^\dagger S_a^\dagger + \bar{S}_a^\dagger H_a^\dagger)J\rangle + \text{H.c.} \tag{5}$$

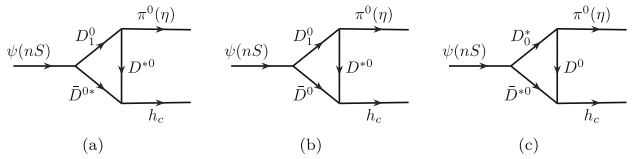

Fig. 2 The hadron-level diagrams including the neutral charmed mesons $(D_1(2430)^0$ and $D_0^*)$ with $s_l^P = (1/2)^+$. The charged and strange charmed meson loops are similar

Here the coupling constants g_1 and g_1' vary for different n's (see Appendix A). $\bar{H}_a = -\vec{\bar{V}}_a \cdot \vec{\sigma} + \bar{P}_a$ and $\bar{S}_a = -\vec{\bar{V}}_{1a} \cdot \vec{\sigma} + \bar{P}_{0a}^*$ represent the charge conjugated meson fields. Conventionally, $A \overleftrightarrow{\partial} B \equiv A(\vec{\partial} B) - (\vec{\partial} A)B$ and the symbol $\langle \cdots \rangle$ means the trace operation in spinor space.

For the coupling of the orbital excited P-wave charmonium fields to the charmed mesons, we have

$$\mathcal{L}_{h_c} = \mathrm{i}\frac{g_2}{2}\langle h_c^{\dagger i} H_a \sigma^i \bar{H}_a \rangle + \mathrm{H.c.}\,, \tag{6}$$

where $h_c^{\dagger i}$ creates the h_c state. The coupling constant $g_2 = -4.2\ \mathrm{GeV}^{1/2}$ [20] was kept unchanged throughout the present work.

By means of the heavy meson chiral perturbation theory, the leading order Lagrangian coupling the light mesons π^0 or η to the charmed meson pair is

$$\mathcal{L}_\phi = -\frac{g}{2}\langle H_a^\dagger H_a \vec{\sigma} \cdot \vec{u}_{aa} \rangle + \mathrm{i}\frac{g'}{2}\langle H_a^\dagger S_a u_{aa}^0 \rangle\,. \tag{7}$$

Here the coupling constant g is known to be 0.6. $\vec{u} = -\sqrt{2}\vec{\partial}\phi/F_\pi + c\phi^3$ and $u^0 = -\sqrt{2}\partial^0\phi/F_\pi$, where $F_\pi = 92.4$ MeV is the pion decay constant in the chiral limit. ϕ denotes the pseudoscalar fields represented by

$$\phi = \begin{pmatrix} \frac{\pi^0}{\sqrt{2}} + \frac{\beta\eta + \gamma\eta'}{\sqrt{2}} & \pi^+ & K^+ \\ \pi^- & -\frac{\pi^0}{\sqrt{2}} + \frac{\beta\eta + \gamma\eta'}{\sqrt{2}} & K^0 \\ K^- & \bar{K}^0 & -\gamma\eta + \beta\eta' \end{pmatrix}, \tag{8}$$

where the physical states η and η' are generally considered as the mixtures of the flavor eigenstates [25,41–44]:

$$\begin{aligned} |\eta\rangle &= \beta|n\bar{n}\rangle - \gamma|s\bar{s}\rangle\,, \\ |\eta'\rangle &= \gamma|n\bar{n}\rangle + \beta|s\bar{s}\rangle\,, \end{aligned} \tag{9}$$

with $|n\bar{n}\rangle \equiv (|u\bar{u}\rangle + |d\bar{d}\rangle)/\sqrt{2}$. The parameters $\beta = \cos\alpha$ and $\gamma = \sin\alpha$, where $\alpha = \theta_P + \arctan\sqrt{2}$ with the pseudoscalar mixing angle θ_P ranging from $-24.6°$ to $-11.5°$ (see Ref. [4] and references therein).

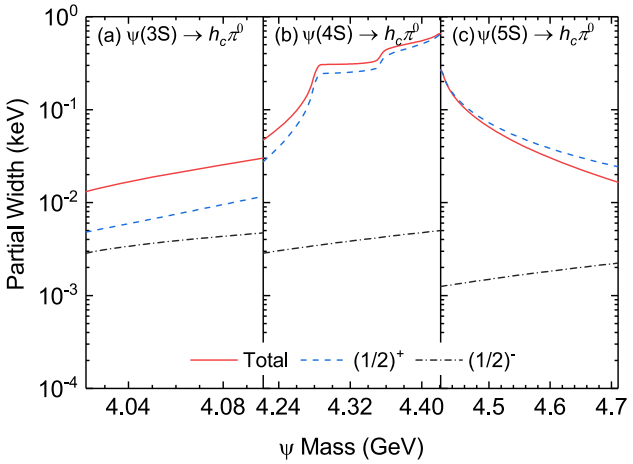

Fig. 3 The partial widths of the different radial excited charmonia $\psi(3S)$ (**a**), $\psi(4S)$ (**b**), and $\psi(5S)$ (**c**) decaying into h_c and π^0. The black dash-dotted lines describe the widths contributed only from the loops made of charmed mesons of $s_l^P = (1/2)^-$, while the blue dashed lines represent the results only by the loops involving $D_1(2430)^0$ or D_0^* mesons with $s_l^P = (1/2)^+$. The red lines are the total partial widths including all the loops

3 Results and discussion

In Fig. 3, we show the partial widths of $\psi(nS) \to h_c\pi^0$. It is known that different theoretical models predict various masses of the S state charmonia. Consequently, we assign a range of masses to $\psi(nS)$ according to the theoretical predictions [45–52], which cover most of the 1^{--} charmonia.

3.1 Partial width of $\psi(nS) \to h_c\pi^0$

Transitions $\psi(nS) \to h_c\pi^0$ break the isospin symmetry. As a result, the amplitudes are given by the differences of the neutral and charged charmed meson loops, which are formulated mathematically in Eqs. (B6) and (B7). In Fig. 3 we show the partial decay widths contributed from the $s_l^P = (1/2)^-$ (dash-dotted line) and $s_l^P = (1/2)^+$ (dashed line) meson loops. The total widths result from all possible loops are depicted by the solid line.

It is noticeable that the partial decay widths for $\psi(3S, 4S, 5S) \to h_c\pi^0$ are dominated by the loops involving the $s_l^P = (1/2)^+$ charmed mesons. The partial widths contributed from the loops in Fig. 1 and those like them that are made of the $s_l^P = (1/2)^-$ charmed mesons are of order 10^{-3}–10^{-2} keV, while they are around 0.1–10 keV from those loops in Fig. 2. This finding is plausible in view of the fact that all the vertex couplings for the loops involving the $s_l^P = (1/2)^+$ charmed mesons can happen in an S-wave, while the pion vertex and the initial charmonium vertex in Fig. 1 and the analogue have to be in a P-wave. A semi-quantitative estimation of the importance of the loops

involving the $s_l^P = (1/2)^+$ charmed mesons using the power counting scheme [8,20,21] is given in Appendix C.

It is recalled that the contribution to the amplitude of the $\psi(2\,S) \to h_c\pi^0$ from the $s_l^P = (1/2)^-$ charmed meson loops is strongly suppressed due to the small phase spaces [20,21]. The partial width for the $\psi(3\,S, 4\,S, 5\,S) \to h_c\pi^0$ from the $s_l^P = (1/2)^-$ charmed meson loops was calculated to be around 10^{-3}–10^{-2} keV, more than two orders of magnitude larger than the cases for the $\psi(2S)$ (about 10^{-5} keV [20,21]). The weakened suppression can be attributed to the large phase spaces of the present transitions of the higher radial excited charmonia $\psi(3S, 4S, 5S)$ with greater mass.

As seen from Fig. 3a the partial width of the $\psi(3\,S) \to h_c\pi^0$ remains nearly constant in the mass range considered. The $\psi(4040)$ with a full width of 80 MeV [4] is widely accepted as the $\psi(3\,S)$. It yields a branching ratio of the order of 2.1×10^{-7} for the $\psi(3\,S) \to h_c\pi^0$. For the $\psi(4S)$, the partial decay width increases from 0.05 keV to 0.7 keV with increasing the mass. Moreover, the curve shows two steps at the mass of 4.28 GeV and 4.35 GeV. These two values are close to the thresholds of the $D_1\bar{D}$ and $D_0^*\bar{D}^*$. The theoretical model calculations [46,47] suggest both $\psi(4230)$ and $\psi(4415)$ to be $\psi(4S)$. In view of the widths of the $\psi(4230)$ and $\psi(4415)$ [4], it yields branching ratios of $\sim 1 \times 10^{-6}$ and 1×10^{-5}, respectively.

For the $\psi(5S)$, we consider the masses ranging from 4.421 GeV to 4.711 GeV based on the theoretical predictions [45–52], which is larger than the threshold of the $D_1\bar{D}^*$, i.e., $\sim$ 4.42 GeV. Consequently, the partial width for the transition $\psi(5S) \to h_c\pi^0$ decreases as the mass goes away from the threshold. It is seen that the partial width decreases monotonically from about 0.3–0.02 keV with increasing the mass. Either of the two resonances $\psi(4415)$ and $\psi(4660)$ could be considered as $\psi(5S)$ based on the predictions of different theoretical models [45,46]. Combining our results and the world average widths of 62 and 72 MeV for the $\psi(4415)$ and $\psi(4660)$ [4], we get the branching ratios of $\sim 4 \times 10^{-6}$ and $\sim 3.5 \times 10^{-7}$, respectively.

3.2 Partial width of $\psi(nS) \to h_c\eta$

For the transitions $\psi(nS) \to h_c\eta$, they do not break isospin symmetry, but suffer violation of the SU(3) symmetry. In this case, the amplitudes can be described by the differences between the charmed-nonstrange and charmed-strange meson loops as in Eqs. (B8) and (B9).

We exhibit in Fig. 4 the partial widths of the processes $\psi(3S, 4S, 5S) \to h_c\eta$, which follow the different mass dependence from the $\psi(3\,S, 4\,S, 5\,S) \to h_c\pi^0$, especially for the $\psi(4\,S\,, 5\,S)$. The results were obtained using the η-η' mixing angle of $-19.1°$, which was determined experimentally [53]. In the mass range we considered, the partial widths vary between 0.1 and 100 keV. Obviously, the partial widths are also mainly contributed from the loops made of the $s_l^P = (1/2)^+$ mesons, although the $s_l^P = (1/2)^-$ meson loops give rise to relatively large contributions for the $\psi(4S, 5S) \to h_c\eta$ due to the isospin symmetry in comparison with the case of the pion emission (see Fig. 3). For the case of $\psi(3\,S) \to h_c\eta$, the rather small contribution from the $s_l^P = (1/2)^-$ charmed meson loops results from the small phase space.

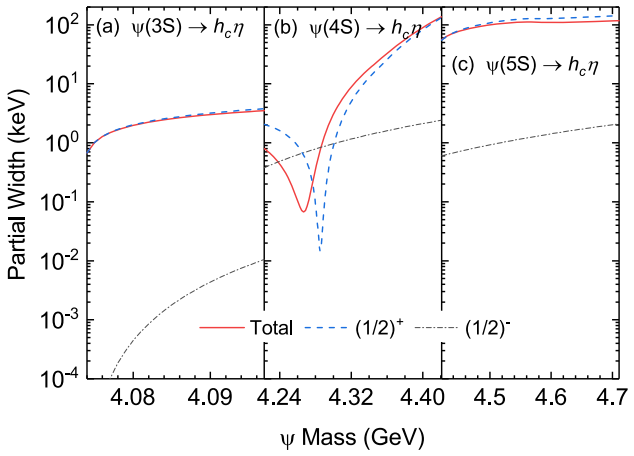

Fig. 4 The partial widths for $\psi(3\,S, 4\,S, 5\,S) \to h_c\eta$. The representations of the different lines are analogous to those in the caption of Fig. 3. The calculations were performed using the η-η' mixing angle of $\theta_P = -19.1°$ [53]

If the $\psi(3S)$ has a mass larger than the threshold of h_c and η, i.e., 4.073 GeV, we could observe a partial width of about 1 keV. However, there is no experimental observation of the 1^{--} $c\bar{c}$ states in the mass range between 4.073 and 4.100 GeV. It is noted that the total width for the transition $\psi(4\,S) \to h_c\eta$ shows a minimum. This minimum is caused by the contribution of the meson loops including the D_1 or D_0^*. For the $\psi(4230)$ and $\psi(4415)$, which favor the $\psi(4S)$ states [45–47], our numerical results predict branching ratios of about 1.6×10^{-5} and 2.2×10^{-3}, respectively. For the $\psi(5S)$ state, corresponding possibly to the experimental observations of the $\psi(4415)$ and $\psi(4660)$, it yields branching ratios of 9×10^{-4} and 1.5×10^{-3}, respectively.

In Fig. 5 we plot the partial widths for the $\psi(4415)$ and $\psi(4660)$ as a function of the η–η' mixing angle θ_P. In calculations, the mixing angle θ_P was assumed to be varied from $-24.6°$ to $-11.5°$ [4]. Moreover, we selected the $\psi(4415)$ and $\psi(4660)$ to be $\psi(4\,S)$ and $\psi(5\,S)$, respectively, based on the model predictions [46]. It is clearly seen that the partial decay widths for $\psi(4\,S)$ and $\psi(5\,S)$ both decrease with increasing the mixing angle.

4 Summary

We have presented the partial widths for the higher radial excited charmonia $\psi(nS)$ decaying into the orbital excited

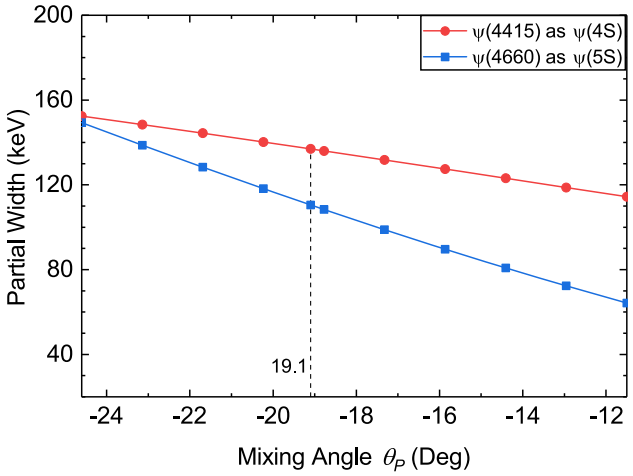

Fig. 5 The partial decay widths for $\psi(4\,S\,,5\,S) \to h_c\eta$ with the η–η' mixing angle. The $\psi(4S)$ is taken to be the $\psi(4415)$ and the $\psi(4660)$ is assigned to be the $\psi(5S)$. The solid lines are only to guide the eye

charmonium h_c and the pion or eta meson. The widths were calculated using the nonrelativistic effective field theory. In the calculations, we considered only the contributions from the loops made of the intermediate charmed mesons. The results indicate that the partial widths for the transitions $\psi(nS) \to h_c\pi^0$ are dominated by the loops involving the charmed mesons with $s_l^P = (1/2)^+$, whereas the $s_l^P = (1/2)^-$ charmed meson loop contributions are of minor importance.

For the transitions $\psi(3S, 4S, 5S) \to h_c\pi^0$, the partial widths are of the order of 0.01–1 keV, whereas the partial widths of the processes $\psi(3S, 4S, 5S) \to h_c\eta$ are found to be between 0.1 keV and 100 keV. In view of the experimental measurements for the full widths of the possible S-state charmonia [4], for instance the $\psi(4040)$, $\psi(4415)$, and $\psi(4660)$ usually known as $\psi(3\,S)$, $\psi(4S)$, and $\psi(5S)$, respectively, the partial widths for $\psi(3S, 4S, 5S) \to h_c\pi^0$ correspond to branching ratios on the order of 10^{-7}, 10^{-5}, and 10^{-7}, while the branching ratios for $\psi(4\,S, 5\,S) \to h_c\eta$ are 10^{-3} when the masses of the $4S$ and $5S$ charmonia are higher than $\psi(4415)$. Moreover, it is indicated that the partial widths for the transitions $\psi(4S, 5S) \to h_c\eta$ decrease as the η-η' mixing angle increases. We found that the branching ratios for $\psi(nS) \to h_c\pi^0(\eta)$ exhibit maxima near $\psi(4415)$ mass. The $\psi(4415)$ is generally supposed to be the $\psi(4S)$ state in literature. As a result, it is more likely to observe these two processes in the $\psi(4415)$ decays. Furthermore, more and more data in the higher charmonia energy region can be expected in the BESIII and Belle-II experiments.

Acknowledgements Particular thanks are devoted to Fengkun Guo for providing us the numerical computation program. We thank Jujun Xie and Qi Wu for helpful discussions. This work is supported by the National Natural Science Foundation of China under Grants no. 12105153, no. 12075133, no. 12047503 and by the Natural Science Foundation of Shandong Province under Grant no. ZR2021MA082 and No. ZR2022ZD26. It is also partly supported by Taishan Scholar Project of Shandong Province (Grant no. tsqn202103062) and the Higher Educational Youth Innovation Science and Technology Program Shandong Province (Grant no. 2020KJJ004).

Data Availability This manuscript has no associated data or the data will not be deposited. [Authors' comment: All the relevant data are already contained in the manuscript.]

Funded by SCOAP^3. SCOAP^3 supports the goals of the International Year of Basic Sciences for Sustainable Development.

Appendix A: The coupling constants g_1, g_1', and g'

In order to obtain the coupling constants g_1 and g_1' involving the $\psi(nS)$ and D mesons, we use the two-body decays of $\psi(nS)$ into the $D\bar{D}$ pair and the $D_1\bar{D}^0$ pair, whose partial decay widths have been theoretically predicted in Ref. [45]. From the Lagrangian in Eq. (5), the widths for the foregoing decays are

$$\begin{aligned}\Gamma(\psi \to D\bar{D}) &= \frac{g_1^2}{6\pi}\frac{M_D^2}{M_\psi}|\vec{q}|^3\,,\\ \Gamma(\psi \to D_1\bar{D}^0) &= \frac{g_1'^2}{2\pi}\frac{M_{D_1}M_{D^0}}{M_\psi}|\vec{q}|\,,\end{aligned} \tag{A1}$$

where $\vec{q}$ is the momentum of some D meson in the final states. Using the theoretical decay widths for the processes $\psi(3\,S, 4\,S, 5\,S) \to D\bar{D}$ calculated in linear and screened potential models [45], we estimate the coupling constant $g_1 = 0.28$, 0.17, and 0.085 GeV$^{-3/2}$ for $\psi(3\,S)$, $\psi(4S)$, and $\psi(5S)$, respectively. These values are consistent with Guo's estimation [20,21,54] that the coupling constant g_1 seems to decrease as n increases and to become less than 1 for $n > 3$.

Similarly, we get $g_1' = 0.42$ GeV$^{-1/2}$ for $\psi(4\,S)$ and 0.27 GeV$^{-1/2}$ for $\psi(5\,S)$. Since the threshold of the process $\psi \to D_1\bar{D}^0$ exceeds all predicted masses of the $\psi(3S)$, we cannot directly estimate the coupling constant from the decay width. Therefore, we assume ${g_1'}^2(3\,S)/{g_1'}^2(4\,S) \simeq {g_1}^2(3\,S)/{g_1}^2(4\,S)$ and get $g_1' = 0.69$ GeV$^{-1/2}$ for $\psi(3S)$.

To estimate the coupling constant g', the full width of the particles $D_1(2340)^0$ and D_0^* were assumed to be saturated by the processes $D_1^0 \to D^*\pi$ and $D_0^* \to D\pi$, respectively. The relevant widths are [40]

$$\Gamma(D_1^0 \to D^*\pi) = \frac{3g'^2}{8\pi F_\pi^2}\frac{M_{D^*}}{M_{D_1^0}}\left(M_\pi^2 + |\vec{q}_\pi|^2\right)|\vec{q}_\pi|\,,$$
$$\Gamma(D_0^* \to D\pi) = \frac{3g'^2}{8\pi F_\pi^2}\frac{M_{D}}{M_{D_0^*}}\left(M_\pi^2 + |\vec{q}_\pi|^2\right)|\vec{q}_\pi|\,. \quad \text{(A2)}$$

Using $\Gamma = 314$ MeV for $D_1(2340)^0$ [4], we get $|g'| = 0.74$. Likewise, it follows $|g'| = 0.52$ for D_0^* with $\Gamma = 229$ MeV. In present calculations, we take the average value of $g' = 0.63$.

Appendix B: Amplitudes of $\psi(nS) \to h_c\pi^0(\eta)$

Here we use the so-called vector loop integral introduced by Guo [21] to describe the amplitudes governed by the Lagrangians in the foregoing section. In the initial charmonium frame the vector loop is defined as

$$q^i I^{(1)} \equiv \mathrm{i}\int \frac{\mathrm{d}^d l}{(2\pi)^d}\frac{l^i}{D_1 D_2 D_3}\,, \quad \text{(B1)}$$

where $D_1 = l^2 - m_1^2 + \mathrm{i}\epsilon$, $D_2 = (p-l)^2 - m_2^2 + \mathrm{i}\epsilon$, and $D_3 = (l-q)^2 - m_3^2 + \mathrm{i}\epsilon$. m_1, m_2, and m_3 are the mass of the intermediate charmed mesons in the triangular loops shown in Figs. 1 and 2, and l, $(p-l)$, and $(l-q)$ are their four-momenta. Note that p represents the four-momentum of the initial particle and q is the four-momentum of the light meson in the final states, i.e., the pion or eta meson. Using the technique of tensor reduction, the vector loop can be written in the analytic form [21]

$$I^{(1)} = \frac{\mu_{23}}{am_3}\left[B(c'-a) - B(c) + \frac{1}{2}(c'-c)I(q)\right]. \quad \text{(B2)}$$

Here $I(q)$ is the three-point scalar loop function. In the nonrelativistic framework, we have [21]

$$I(q) = \frac{\mu_{12}\mu_{23}}{16\pi m_1 m_2 m_3}\frac{1}{\sqrt{a}}\left[\arctan\left(\frac{c'-c}{2\sqrt{ac}}\right) + \arctan\left(\frac{2a+c-c'}{2\sqrt{a(c'-a)}}\right)\right]. \quad \text{(B3)}$$

Moreover, the function $B(c)$ is defined as

$$B(c) = -\frac{\mu_{12}\mu_{23}}{16\pi m_1 m_2 m_3}\sqrt{c-\mathrm{i}\epsilon}\,. \quad \text{(B4)}$$

The parameters μ_{ij}, a, c, and c' in Eqs. (B2)–(B4) are defined as [21]

$$\mu_{ij} = \frac{m_i m_j}{m_i + m_j}, \quad a = \left(\frac{\mu_{23}}{m_3}\right)^2\vec{q}^2,$$
$$c = 2\mu_{12}(m_1 + m_2 - M),$$
$$c' = 2\mu_{23}(m_2 + m_3 + q^0 - M) + \frac{\mu_{23}}{m_3}\vec{q}^2, \quad \text{(B5)}$$

where M is the mass of the initial particle.

In terms of the integral $I^{(1)}$, the amplitude $\mathcal{M}^{\pi}_{(1/2)^-}$ due to the loops made of charmed mesons with $s_l^P = (1/2)^-$ is

$$\begin{aligned}\mathcal{M}^{\pi}_{(1/2)^-} =& \frac{2gg_1g_2}{F_\pi}\vec{q}^2\vec{\varepsilon}(\psi)\cdot\vec{\varepsilon}(h_c)\\ &\times\Big[I^{(1)}(D^{*0},\bar{D}^0,D^{*0}) - I^{(1)}(D^{*0},\bar{D}^{*0},D^{*0})\\ &+ I^{(1)}(D^{*0},\bar{D}^{*0},D^0) - I^{(1)}(D^0,\bar{D}^{*0},D^{*0})\\ &- I^{(1)}(D^{*+},D^-,D^{*+}) + I^{(1)}(D^{*+},D^{*-},D^{*+})\\ &- I^{(1)}(D^{*+},D^{*-},D^+) + I^{(1)}(D^+,D^{*-},D^{*+})\Big]\\ &+ \frac{2gg_1g_2}{F_\pi}\vec{q}\cdot\vec{\varepsilon}(\psi)\vec{q}\cdot\vec{\varepsilon}(h_c)\\ &\times\Big[I^{(1)}(D^0,\bar{D}^0,D^{*0}) - I^{(1)}(D^{*0},\bar{D}^0,D^{*0})\\ &+ I^{(1)}(D^0,\bar{D}^{*0},D^{*0}) - I^{(1)}(D^{*0},\bar{D}^{*0},D^{*0})\\ &- I^{(1)}(D^+,D^-,D^{*+}) + I^{(1)}(D^{*+},D^-,D^{*+})\\ &- I^{(1)}(D^+,D^{*-},D^{*+}) + I^{(1)}(D^{*+},D^{*-},D^{*+})\Big].\end{aligned} \quad \text{(B6)}$$

Note that the variables D's of the function $I^{(1)}$ not only indicate the mesons forming the loops but also serve as the corresponding charmed meson masses. For the loops involving the charmed mesons with $s_l^P = (1/2)^+$, i.e., the loops in Fig. 2 and the analogue, the amplitude is

$$\begin{aligned}\mathcal{M}^{\pi}_{(1/2)^+} =& \mathrm{i}\frac{g'g_1'g_2}{F_\pi}E_\pi\vec{\varepsilon}(\psi)\cdot\vec{\varepsilon}(h_c)\Big[I^{(1)}(D_0^*,\bar{D}^{*0},D^0)\\ &+ 2I^{(1)}(D_1^0,\bar{D}^0,D^{*0}) - 4I^{(1)}(D_1^0,\bar{D}^{*0},D^{*0})\\ &- I^{(1)}(D_0^{*+},D^{*-},D^+) - 2I^{(1)}(D_1^+,D^-,D^{*+})\\ &+ 4I^{(1)}(D_1^+,D^{*-},D^{*+})\Big],\end{aligned} \quad \text{(B7)}$$

where $E_\pi = \sqrt{\vec{q}^2 + M_\pi^2}$ is the pion energy in the rest frame of the initial charmonium.

However, the amplitude of the transition $\psi \to h_c\eta$ is somewhat complicated for the loops composed of charmed mesons of $s_l^P = (1/2)^-$ state due to the charmed-strange mesons. It reads

$$
\begin{aligned}
\mathcal{M}^{\eta}_{(1/2)^-} &= \beta\frac{2gg_1g_2}{F_\pi}\vec{q}^2\vec{\varepsilon}(\psi)\cdot\vec{\varepsilon}(h_c)\\
&\times\Big[I^{(1)}(D^{*0},\bar{D}^0,D^{*0})-I^{(1)}(D^{*0},\bar{D}^{*0},D^{*0})\\
&+I^{(1)}(D^{*0},\bar{D}^{*0},D^0)-I^{(1)}(D^0,\bar{D}^{*0},D^{*0})\\
&+I^{(1)}(D^{*+},D^-,D^{*+})-I^{(1)}(D^{*+},D^{*-},D^{*+})\\
&+I^{(1)}(D^{*+},D^{*-},D^+)-I^{(1)}(D^+,D^{*-},D^{*+})\Big]\\
&+\sqrt{2}\gamma\frac{2gg_1g_2}{F_\pi}\vec{q}^2\vec{\varepsilon}(\psi)\cdot\vec{\varepsilon}(h_c)\\
&\times\Big[I^{(1)}(D_s^+,D_s^{*-},D_s^{*+})-I^{(1)}(D_s^{*+},D_s^{*-},D_s^+)\\
&-I^{(1)}(D_s^{*+},D_s^-,D_s^{*+})+I^{(1)}(D_s^{*+},D_s^{*-},D_s^{*+})\Big]\\
&+\beta\frac{2gg_1g_2}{F_\pi}\vec{q}\cdot\vec{\varepsilon}(\psi)\vec{q}\cdot\vec{\varepsilon}(h_c)\\
&\times\Big[I^{(1)}(D^0,\bar{D}^0,D^{*0})-I^{(1)}(D^{*0},\bar{D}^0,D^{*0})\\
&+I^{(1)}(D^0,\bar{D}^{*0},D^{*0})-I^{(1)}(D^{*0},\bar{D}^{*0},D^{*0})\\
&+I^{(1)}(D^+,D^-,D^{*+})-I^{(1)}(D^{*+},D^-,D^{*+})\\
&+I^{(1)}(D^+,D^{*-},D^{*+})-I^{(1)}(D^{*+},D^{*-},D^{*+})\Big]\\
&+\sqrt{2}\gamma\frac{2gg_1g_2}{F_\pi}\vec{q}\cdot\vec{\varepsilon}(\psi)\vec{q}\cdot\vec{\varepsilon}(h_c)\\
&\times\Big[I^{(1)}(D_s^{*+},D_s^-,D_s^{*+})-I^{(1)}(D_s^+,D_s^-,D_s^{*+})\\
&-I^{(1)}(D_s^+,D_s^{*-},D_s^{*+})+I^{(1)}(D_s^{*+},D_s^{*-},D_s^{*+})\Big].
\end{aligned}
\tag{B8}
$$

Here β and γ, already defined in Eq. (9), are governed by the pseudoscalar mixing angle θ_P. The form of the amplitude from the loops of the $s_l^P=(1/2)^+$ mesons are

$$
\begin{aligned}
\mathcal{M}^{\eta}_{(1/2)^+} &= \mathrm{i}\beta\frac{g'g_1'g_2}{F_\pi}E_\eta\vec{\varepsilon}(\psi)\cdot\vec{\varepsilon}(h_c)\Big[I^{(1)}(D_0^*,\bar{D}^{*0},D^0)\\
&+2I^{(1)}(D_1^0,\bar{D}^0,D^{*0})-4I^{(1)}(D_1^0,\bar{D}^{*0},D^{*0})\\
&+I^{(1)}(D_0^{*+},D^{*-},D^+)+2I^{(1)}(D_1^+,D^-,D^{*+})\\
&-4I^{(1)}(D_1^+,D^{*-},D^{*+})\Big]\\
&-\mathrm{i}\sqrt{2}\gamma\frac{g'g_1'g_2}{F_\pi}E_\eta\vec{\varepsilon}(\psi)\cdot\vec{\varepsilon}(h_c)\Big[I^{(1)}(D_{s0}^{*+},D_s^{*-},D_s^+)\\
&+2I^{(1)}(D_{s1}^+,D_s^-,D_s^{*+})-4I^{(1)}(D_{s1}^+,D_s^{*-},D_s^{*+})\Big].
\end{aligned}
\tag{B9}
$$

Here it should be pointed out that the amplitudes in Eqs. (B6)–(B9) need to be multiplied by the factor $\sqrt{M_\psi M_{h_c}}$ due to the nonrelativistic normalization of the heavy fields in the Lagrangian, where M_ψ and M_{h_c} are the initial and final charmonium, respectively.

Appendix C: Power counting

In order to semiquantitatively evaluate the importance of the loops involving the $(1/2)^+$ charmed mesons as shown in Fig. 2, we here provide the NREFT power counting [8]. Within the framework of NREFT, the amplitudes from those loops made of $(1/2)^-$ charmed mesons like in Fig. 1 scale as [20,21]

$$
\mathcal{M}_{(1/2)^-}\propto\frac{\vec{q}^2}{v_-M_D^2}\frac{1}{v_-^2}. \tag{C1}
$$

For the loops involving the $(1/2)^+$ charmed mesons like in Fig. 2, the corresponding amplitudes scale as

$$
M_{(1/2)^+}\propto\frac{E_\pi}{v_+M_D}\frac{1}{v_+^2}. \tag{C2}
$$

Note that these two scaling laws have included the symmetry breaking [21], which is implied by $1/v^2$. Here $v_\pm$ are regraded as the average velocities of the intermediate charmed mesons in the triangular loops, defined as [8]

$$
v=\frac{1}{2}\left(\frac{\sqrt{|c|}}{2\mu_{12}}+\frac{\sqrt{|c'-a|}}{2\mu_{23}}\right), \tag{C3}
$$

where a, c, c', and μ_{ij} have been defined in Eq. (B5).

In the present case, the momentum $|\vec{q}|$ and the energy E_π are approximately equal as well as the two velocities $v_\pm$. Hence, from Eqs. (C1) and (C3), the importance of the $(1/2)^+$ charmed meson loops is roughly indicated by the factor $M_D/|\vec{q}|>1$. In a detailed manner, taking Figs. 1a and 2a as examples, we get $v_-=0.41$, $v_+=0.38$, $|\vec{q}|=464$ MeV, and $E_\pi=483$ MeV for $\psi(4040)\to h_c\pi^0$. Therefore, it yields $\mathcal{M}_{(1/2)^+}/\mathcal{M}_{(1/2)^-}\sim\mathcal{O}(5)$. For $\psi(4415)\to h_c\pi^0$, the amplitude ratio $\mathcal{M}_{(1/2)^+}/\mathcal{M}_{(1/2)^-}\sim\mathcal{O}(10)$. The power counting for the transitions with eta emission is similar. These rough estimations could indicate the importance of the loops involving the $(1/2)^+$ charmed mesons.

References

1. N. Brambilla, M. Krämer, R. Mussa et al., Heavy quarkonium physics (2005). arxiv:hep-ph/0412158
2. E. Eichten, S. Godfrey, H. Mahlke, J.L. Rosner, Rev. Mod. Phys. **80**, 1161 (2008)
3. N. Brambilla, S. Eidelman, B.K. Heltsley et al., Eur. Phys. J. C **71**, 1534 (2011)
4. R.L. Workman et al., Prog. Theor. Exp. Phys. **2022**, 083C01 (2022)
5. S.F. Radford, W.W. Repko, Phys. Rev. D **75**, 074031 (2007)
6. A.V. Manohar, Introduction to effective field theories (2018). arXiv:1804.05863 [hep-ph]
7. G. Münster, M. Walzl, Lattice gauge theory: a short primer (2000). arXiv:hep-lat/0012005

8. F.-K. Guo, C. Hanhart, U.-G. Meißner, Q. Wang, Q. Zhao, B.-S. Zou, Rev. Mod. Phys. **90**, 015004 (2018)
9. N. Brambilla, S. Eidelman, C. Hanhart, A. Nefediev, C.-P. Shen, C.E. Thomas, A. Vairo, C.-Z. Yuan, Phys. Rep. XYZ States Exp. Theor. Status Perspect. **873**, 1 (2020)
10. X. Liu, X.-Q. Zeng, X.-Q. Li, Phys. Rev. D **74**, 074003 (2006)
11. G. Li, Q. Zhao, B.-S. Zou, Phys. Rev. D **77**, 014010 (2008)
12. G. Li, Q. Zhao, Phys. Lett. B **670**, 55 (2008)
13. Y.-J. Zhang, G. Li, Q. Zhao, Phys. Rev. Lett. **102**, 172001 (2009)
14. X. Liu, B. Zhang, X.-Q. Li, Phys. Lett. B **675**, 441 (2009)
15. Z. Yuan-Jiang, L. Gang, Z. Qiang, Chin. Phys. C **34**, 1181 (2010)
16. D.-Y. Chen, J. He, X.-Q. Li, X. Liu, Phys. Rev. D **81**, 074006 (2010)
17. Q. Zhao, Nuclear Physics B-Proceedings Supplements Proceedings of the QCD 10: 15th High-Energy Physics International Conference
18. D.-Y. Chen, Y.-B. Dong, X. Liu, Eur. Phys. J. C **70**, 177 (2010)
19. F.-K. Guo, C. Hanhart, U.-G. Meißner, Phys. Rev. Lett. **103**, 082003 (2009)
20. F.-K. Guo, C. Hanhart, G. Li, U.-G. Meißner, Q. Zhao, Phys. Rev. D **82**, 034025 (2010)
21. F.-K. Guo, C. Hanhart, G. Li, U.-G. Meißner, Q. Zhao, Phys. Rev. D **83**, 034013 (2011)
22. Z. Cao, M. Cleven, Q. Wang, Q. Zhao, Eur. Phys. J. C **76**, 601 (2016)
23. G. Li, Q. Zhao, Phys. Rev. D **84**, 074005 (2011)
24. F.-K. Guo, U.-G. Meißner, Phys. Rev. Lett. **108**, 112002 (2012)
25. G. Li, X.-H. Liu, Q. Wang, Q. Zhao, Phys. Rev. D **88**, 014010 (2013)
26. D.-Y. Chen, X. Liu, T. Matsuki, Phys. Rev. D **91**, 094023 (2015)
27. D.-Y. Chen, X. Liu, T. Matsuki, Prog. Theor. Exp. Phys. **2015**, 043B05 (2015)
28. Q. Wu, G. Li, Y. Zhang, Eur. Phys. J. C **77**, 336 (2017)
29. W.-H. Qin, C.-S. An, G. Li, C. Wang, Y. Wang, Eur. Phys. J. C **79**, 757 (2019)
30. Y. Wang, Q. Wu, G. Li, J.-J. Xie, C.-S. An, Eur. Phys. J. C **80**, 475 (2020)
31. Q. Huang, J.-Z. Wang, R.-G. Ping, X. Liu, Phys. Rev. D **103**, 096006 (2021)
32. R.-Q. Qian, J.-Z. Wang, X. Liu, T. Matsuki, Phys. Rev. D **104**, 094001 (2021)
33. J.-Z. Wang, X. Liu, Phys. Rev. D **107**, 054016 (2023)
34. Z. Qiang, L. Gang, C. Chao-Hsi, Chin. Phys. C **34**, 299 (2010)
35. L. Xue-Qian, Chin. Phys. C **34**, 267 (2010)
36. G. Li, X.-H. Liu, Phys. Rev. D **88**, 094008 (2013)
37. G. Li, C.-S. An, P.-Y. Li, D. Liu, X. Zhang, Z. Zhou, Chin. Phys. C **39**, 063102 (2015)
38. B. Wang, H. Xu, X. Liu, D.-Y. Chen, S. Coito, E. Eichten, Front. Phys. **11**, 111402 (2016)
39. X.-Y. Wang, Z.-X. Cai, G. Li, S.-D. Liu, C.-S. An, J.-J. Xie, Eur. Phys. J. C **83**, 186 (2023)
40. Q. Wu, D.-Y. Chen, F.-K. Guo, Phys. Rev. D **99**, 034022 (2019)
41. Q. Wu, Y. Zheng, S. Liu, G. Li, Phys. Rev. D **107**, 034028 (2023)
42. Q. Wang, G. Li, Q. Zhao, Phys. Rev. D **85**, 074015 (2012)
43. C. Amsler, F.E. Close, Phys. Rev. D **53**, 295 (1996)
44. J.L. Rosner, Phys. Rev. D **27**, 1101 (1983)
45. L.-C. Gui, L.-S. Lu, Q.-F. Lü, X.-H. Zhong, Q. Zhao, Phys. Rev. D **98**, 016010 (2018)
46. Z. Zhao, K. Xu, N. Tagsinsit, A. Kaewsnod, X. Liu, A. Limphirat, W. Sreethawong, K. Khosonthongkee, S. Cheedket, Y. Yan, Mass spectrum of 1-heavy quarkonium (2023). arXiv:2304.06243 [hep-ph]
47. W.-J. Deng, H. Liu, L.-C. Gui, X.-H. Zhong, Phys. Rev. D **95**, 034026 (2017)
48. T. Barnes, S. Godfrey, E.S. Swanson, Phys. Rev. D **72**, 054026 (2005)
49. S. L.Olsen, Front. Phys. **10**, 121 (2015). arXiv:1411.7738 [hep-ex, physics:hep-ph, physics:nucl-ex, physics:nucl-th]
50. D. Molina, M. De Sanctis, C. Fernández-Ramírez, Phys. Rev. D **95**, 094021 (2017)
51. R.F. Lebed, R.E. Mitchell, E.S. Swanson, Prog. Part. Nucl. Phys. **93**, 143 (2017)
52. V. Kher, A.K. Rai, Chin. Phys. C **42**, 083101 (2018)
53. DM2 Collaboration, J. Jousset, Z. Ajaltouni, A. Falvard, H. Jnad, B. Michel, J. C. Montret, D. Bisello, G. Busetto, A. Castro, L. Pescara, F. Racioppi, P. Sartori, L. Stanco, J.E. Augustin, G. Cosme, F. Couchot, F. Fulda, G. Grosdidier, B. Jean-Marie, V. Lep9 eltier, F. Mane, G. Szklarz, R. Baldini, M. Schioppa, Phys. Rev. D **41**, 1389 (1990)
54. F.-K. Guo, C. Hanhart, U.-G. Meißner, Q. Wang, Q. Zhao, Phys. Lett. B **725**, 127 (2013)